



Recently Active Traces of the Bartlett Springs Fault, California: A Digital Database

By James J. Lienkaemper

Data Series 541

**U.S. Department of the Interior
U.S. Geological Survey**

U.S. Department of the Interior
KEN SALAZAR, Secretary

U.S. Geological Survey
Marcia K. McNutt, Director

U.S. Geological Survey, Reston, Virginia 2010

For product and ordering information:
World Wide Web: <http://www.usgs.gov/pubprod>
Telephone: 1-888-ASK-USGS

For more information on the USGS—the Federal source for science about the Earth,
its natural and living resources, natural hazards, and the environment:
World Wide Web: <http://www.usgs.gov>
Telephone: 1-888-ASK-USGS

Suggested citation:
Lienkaemper, James J., 2010, Recently active traces of the Bartlett Springs Fault, California; a digital
database: U.S. Geological Survey Data Series 541, 10 p. and data [<http://pubs.usgs.gov/ds/541/>].

Any use of trade, product, or firm names is for descriptive purposes only and does not imply
endorsement by the U.S. Government.

Although this report is in the public domain, permission must be secured from the individual
copyright owners to reproduce any copyrighted material contained within this report.

Recently Active Traces of the Bartlett Springs Fault, California: A Digital Database

By James J. Lienkaemper

Introduction

This map shows the location of and evidence for recent movement on active fault traces within the Bartlett Springs Fault Zone, California. The location and recency of the mapped traces is based primarily on geomorphic expression of the fault as interpreted from large-scale aerial photography. In a few places, evidence of fault creep and offset Holocene strata in natural and trench exposures confirm the activity of some of these traces.

This publication is formatted both as a digital database for use within a geographic information system (GIS) and for broader public access as map images that may be browsed or downloaded. The report text describes the types of scientific observations used to make the map, gives references pertaining to the fault and the evidence of faulting, and provides guidance for use of and limitations of the map. Locations along the fault are given by distance along the fault from the north end as defined by the map grid described under methodology below (fig 1.)

The term "recently active fault trace" is defined here as a fault trace that has evidence consistent with movement during the Holocene epoch or approximately the past 10,000 years. The Bartlett Springs Fault (BSF) in this publication describes a system of nearly continuous faulting about 170 km long lying eastward of the San Andreas and Maacama Faults (fig. 1). This system has generally been called the Round Valley Fault (fig. 1, km 0–45) north of Middle Fork Eel River and the Hunting Creek Fault (km 150–170) south of Wilson Valley (Bryant, 1982, 1983). However, this study shows sufficient continuity of the active traces to describe these faults as one fault, notwithstanding significant internal structural discontinuities that are likely to be relevant to its seismic potential. North of km 0 (fig. 1), active faulting of the BSF goes into a pronounced releasing bend, becoming the Lake Mountain Fault of Herd (1978), which I treat as mostly a separate fault and, thus, only a minor part of it was mapped in this investigation. Similarly, the BSF at its southern end becomes the Hunting Creek Fault and it also includes a pronounced releasing bend. However, despite being separated by a 2.5-km-long releasing step, most of Hunting Creek Fault is sufficiently well aligned to the BSF that it needs to be considered as capable of jointly rupturing in large earthquakes (Wesnously, 2008). Thus, for purposes of the earthquake rupture

process, the Hunting Creek Fault needs to be treated as a section of the BSF.

Geologic Setting and Fault Mapping

The BSF is a major branch of the San Andreas Fault system. Like the San Andreas, it is a right-lateral, strike-slip fault, meaning that slip is mainly horizontal, so that objects on the opposite side of the fault from the viewer will move to the viewer's right as slip occurs. For a broad discussion of the basic principles of strike-slip faulting and the relation of the BSF to this larger fault system see Wallace (1990).

Bryant (1993, 2000) thoroughly summarizes the geologic setting and previous mapping of the BSF and evaluates its apparent recency of movement using geomorphic interpretation of aerial photography. The fault mostly lies within the Mesozoic Franciscan assemblage (for example, Jayko and others, 1989); however, it also offsets the Pliocene and Pleistocene Cache Formation near Clear Lake (McLaughlin and others, 1990) and two large basins with significant Quaternary and ongoing deposition, the Round Valley near Covelo (Muir and Webster, 1977) and Gravelly Valley near Lake Pillsbury (Ohlin and others, 2010).

Taylor and Swan (1986) demonstrated the Holocene activity of fault traces in the Lake Pillsbury basin in natural and trench exposures. Bryant (1993) mapped the fault as "Holocene active" at km 64–106 and 160–168 (Hunting Creek Fault, Bryant, 1983).

Detailed (1:12,000-scale, December, 1985) aerial photography flown for the Geomatrix study (Taylor and Swan, 1986) was available for the section of the fault near Lake Pillsbury and was used initially to identify and map active traces. For the present study, new 1:12,000-scale aerial photography was flown along the entire 170-km-long fault zone on March 23, 2009. These new photos became the primary resource for interpretation of fault location and recency, because they were flown in earliest spring when the plant cover was minimal and the sun angle was high enough to penetrate the deepest canyons along the fault trace. The quality of these photos is much higher for our purpose than all previously available photography. Much of the section immediately south of Lake Pillsbury was exposed by recent logging, revealing fault traces previously concealed under tree canopy. The

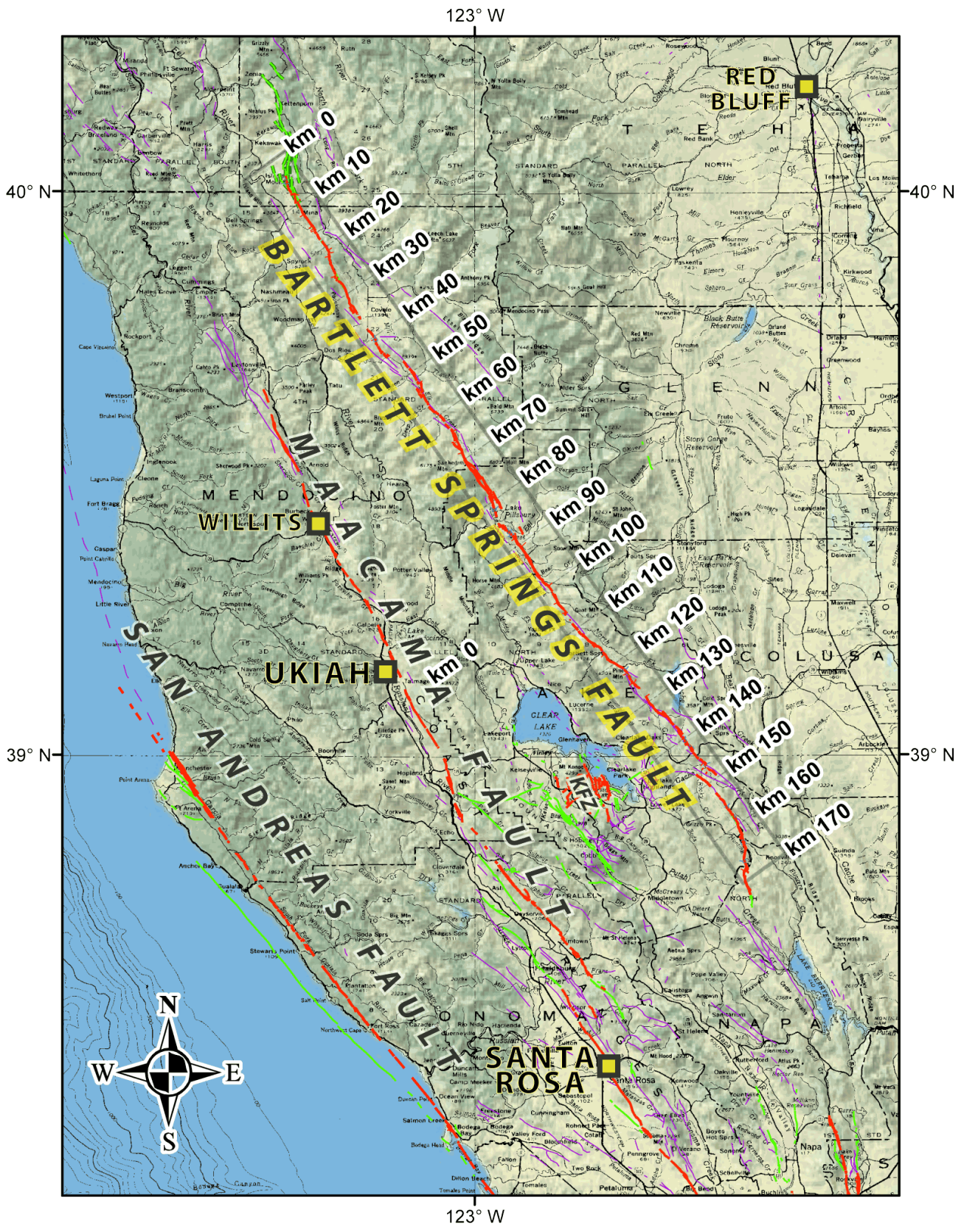


Figure 1. Map showing active traces (red) of the Bartlett Springs Fault and the kilometer grid that is oriented about N. 35.5° W., approximately parallel to the average trend of the fault zone. Other mapped faults are from the Quaternary fault and fold database for the United States (USGS and CGS, 2006) including KFZ (Konocti Fault Zone).

methodology used to interpret the recency and location of fault traces is described in more detail below.

Organization of Digital Files

This mapping has been produced primarily as a digital product to be either used directly as a GIS map layer or to be browsed online at <http://pubs.usgs.gov/ds/541/>. Nontechnical users may gain an overview of the mapping at a resolution of about 1:100,000 or may use virtual globe software at much more detailed resolution.

More technical users may wish to query the GIS database and develop their own map views of the fault using either ArcGIS software (proprietary) or ArcReader (free on internet). As with all GIS data, the reader must be aware of scale limitations of each set of data. Accuracy limits of these data sets will be discussed further below and in the metadata of each GIS file. Documentation of the database fields is

included in the metadata of each GIS file and will not be repeated here.

The projection of all GIS files in the download package is UTM10-WGS84.

Methodology

Map Abbreviations and Kilometer Grid

This fault-strip map takes the approach used by Lienkaemper (1992, 2006) for the Hayward Fault by presenting evidence of fault activity in abbreviated labels (see abbreviation lists, appendix).

For indexing the locations of features discussed in this report, the map includes a kilometer grid oriented along the approximate average strike of the BSF, N. 35.5° W. (fig. 1). The km 0 mark is located in the large releasing bend, where the main active trace of the Lake Mountain Fault deviates distinctly from the average trend of the BSF. The departure of the fault trace of more than 4.5 km off-line from this trend

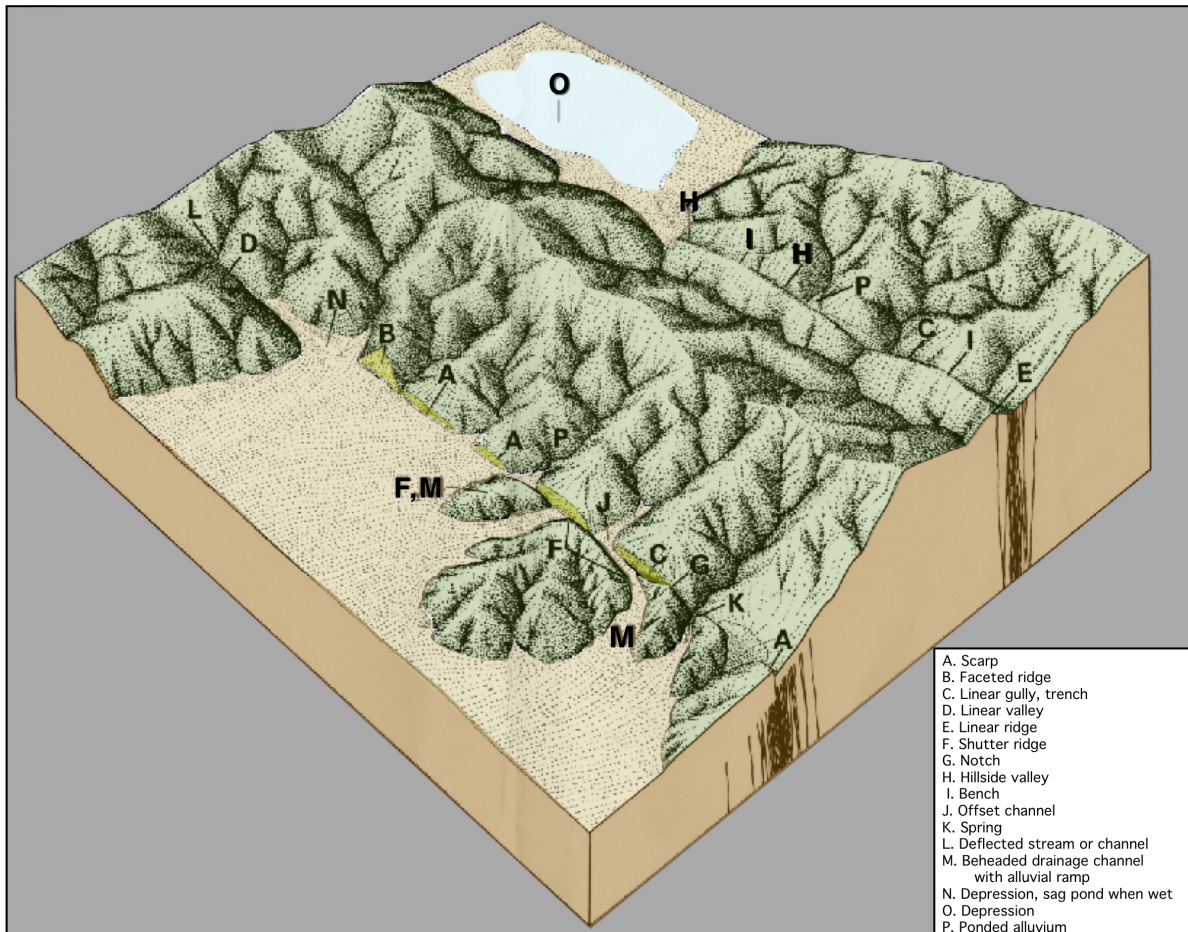


Figure 2. Block diagram showing landforms produced along recently active faults (Sharp, 1972).

may be sufficient to stop most, if not all, through-going ruptures from the north, according to global earthquake rupture data (Wesnousky, 2008), although bilateral ruptures may be able to initiate within this bend. The end of this grid, near km 170, is located at a similar large bend within the Hunting Creek section of the fault. This kilometer grid is available in the GIS data package as a shape file.

Fault Location Inferred from Geomorphic Expression

Geomorphic interpretation, on aerial photographs and in the field, is a critical element in identifying recently active fault traces (Wallace, 1990). The block diagram (fig. 2, after Sharp, 1972) illustrates many of the typical landforms produced by

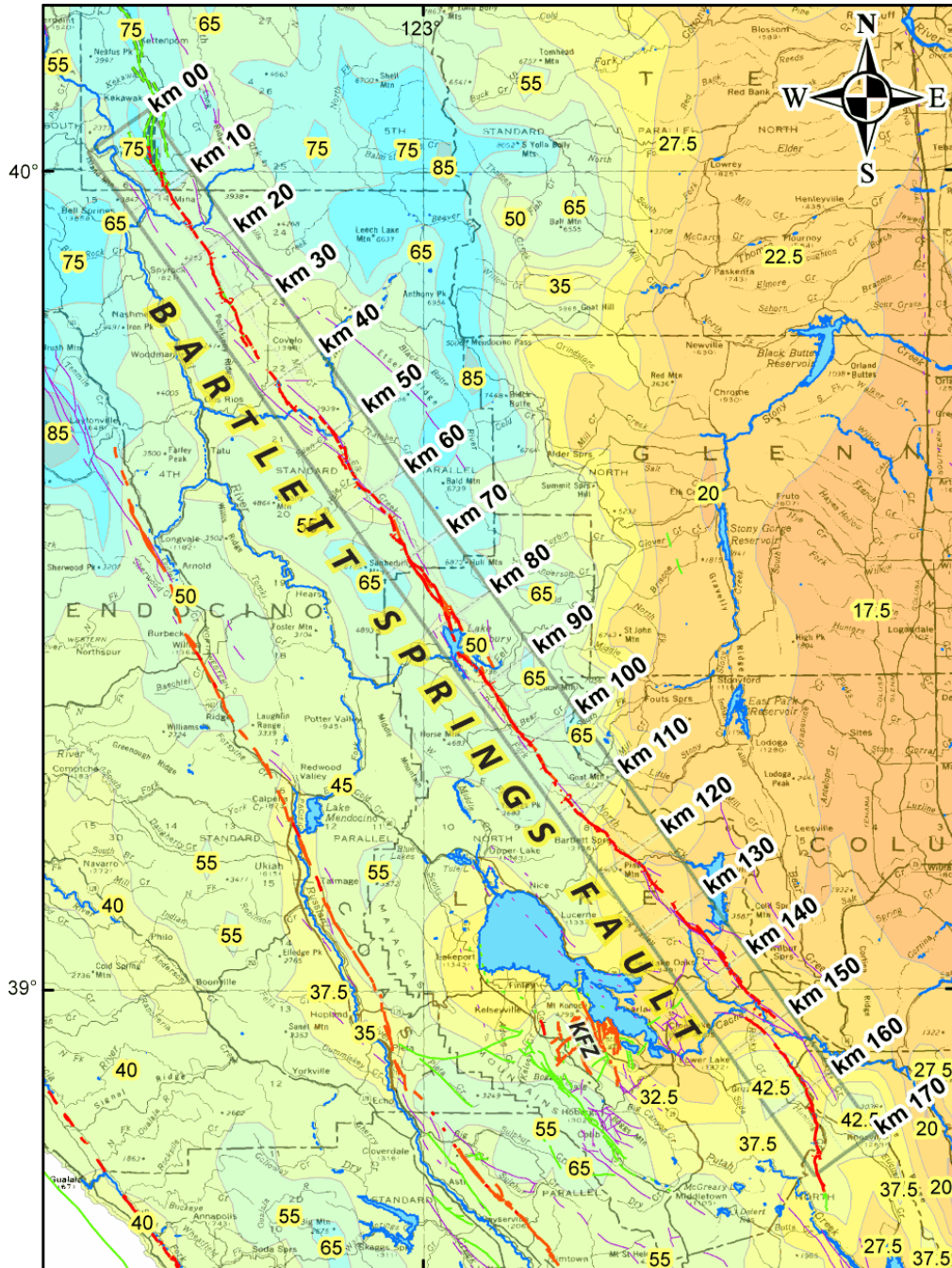


Figure 3. Map showing variation in average annual rainfall (1961–1990) along the Bartlett Springs Fault (average estimated per labeled polygon; from U.S. National Atlas Layer in Daly and Taylor, 2000). Annual rates along the fault vary from a low of approximately 25 in (640 mm) near km 145 to a high of approximately 75 in (1,900 mm). Faults as in Fig. 1.

strike-slip faulting. Most of these geomorphic features result when horizontal sliding along the fault brings different materials into contact at the fault, for example, bedrock against unconsolidated alluvium or colluvium.

The most visible effect is that fault slip causes abrupt disruptions in the natural drainage system, including interrupted subsurface water flow, and results in offset streams and the formation of ponds and springs. Most of the methodology used for this study was already described in Lienkaemper (1992, 2006) for mapping the Hayward Fault, so I will only summarize the main ideas with emphasis on how mapping these two faults may differ.

All rivers and most large streams crossing the BSF are offset right laterally; the largest (and

presumably oldest) drainages show the largest amount of offset (tables 1, 2). For example, the two streams that drain the largest areas, Middle Fork Eel River and Cache Creek, both have drainage basin areas of about 1,400 km² upstream of the fault and are offset 6.6 and 6.2 km, respectively. Offset on drainages northward of km 40 on the BSF does not exceed 1.2 km (North Fork Eel River and Mud, Alder, and Town Creeks) and seems to be limited by the faulting having begun more recently in this area caused by migration of the Mendocino Triple Junction (MTJ; Lock and others, 2006). Smaller offsets (<100 m, table 2) that are most indicative of recent movement were identifiable in only a few places, principally in the driest, southern third of the fault (figs. 3, 4, km 115–170), and were preserved

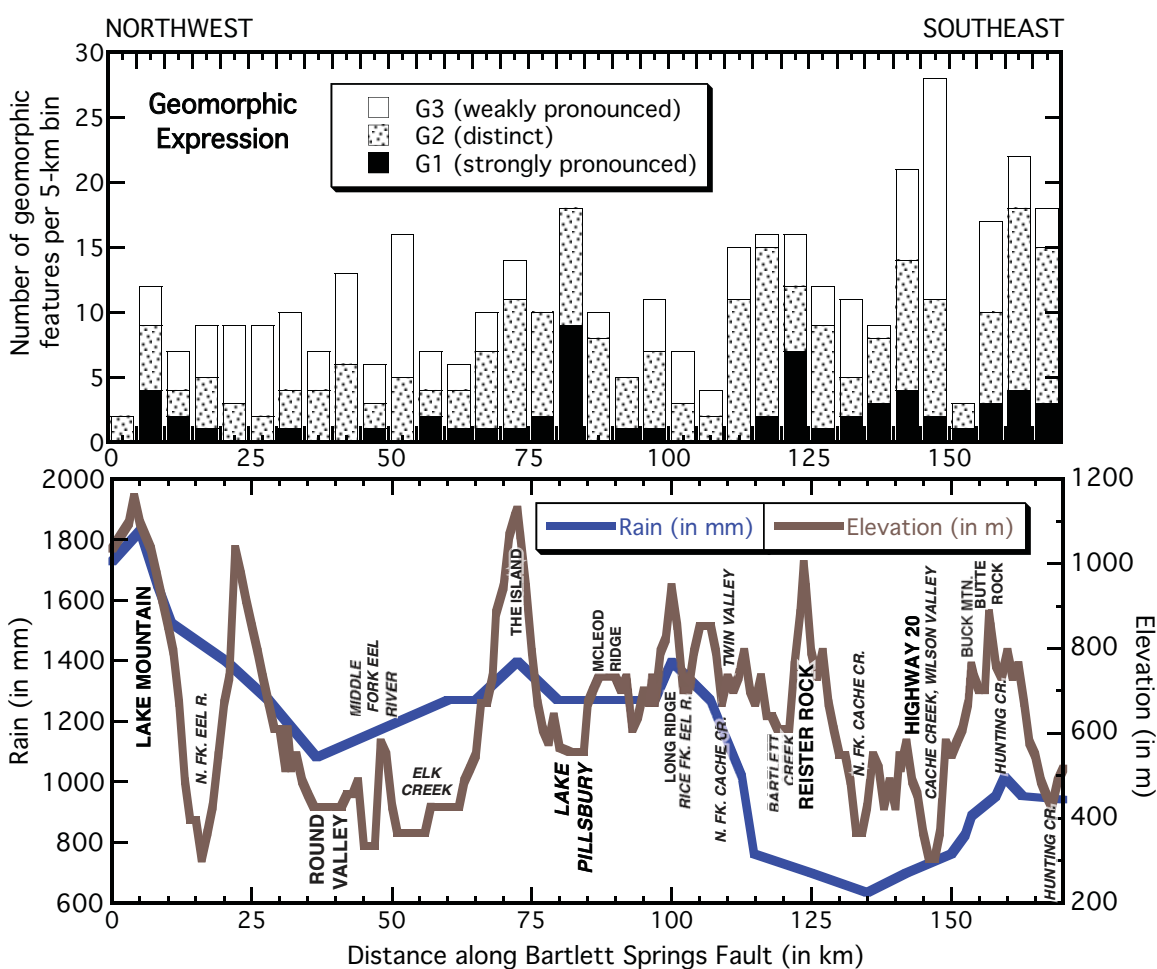


Figure 4. Geomorphic expression and its preservation are controlled by many factors, including, but not limited to, annual rainfall and elevation. Generally, the most strongly pronounced geomorphic features (G1) are found most abundantly along the driest southern third of the fault (km 115–170). However, exceptions occur near Lake Pillsbury (km 81–84), where active deposition and an extensional component of faulting have led to improved development and preservation of features. In contrast, the extremely rapid deposition in Round Valley (km 36–41) appears to eradicate or conceal the active fault traces. Geomorphic features are preserved in ridge-top terrain near Lake Mountain (km 4–8), which has the greatest rainfall along the entire fault (figs. 3, 4, km 115–170), because they are apparently protected from either extreme erosion or deposition. Similarly, in a ridge-top area near Reister Rock (km 122–124), geomorphic features have been especially well preserved.

from erosion on some higher terraces of Elk Creek (km 52–61).

I used a code system (fig. 3; G1, strongly pronounced; G2, distinct; G3, weakly pronounced) to classify my overall judgment about the reliability of geomorphic features for accurately locating recent fault traces. I tried to apply this judgment similarly to previous work, despite considerable differences in rainfall and terrain between the Hayward Fault and BSF (figs. 3, 4). For example, average rainfall along the Hayward Fault (530 mm/yr) is less than half that of BSF (1,130 mm/yr), and the average Hayward Fault elevation is only 80 m compared to 640 m on BSF. The geomorphology of both faults has been degraded historically before earliest aerial photography: on the Hayward mostly by construction of roads and housing and on the BSF by extensive logging.

I identified nearly twice the density of features on the Hayward Fault (4.3 features/km; Lienkaemper, 1992, 2006) compared to the BSF (2.3 features/km; this study). Figure 4 shows that many distinct (G1) features are found in the driest southern third of the fault as expected; however, other clusters of distinct features, such as those at Lake Pillsbury (km 80–84), appear to survive because of good preservation in Pleistocene and younger alluvium. However, in Round Valley (km 35–41), preservation is poorer because features are rapidly buried by alluvium. Overall, the Hayward Fault had a somewhat greater proportion of well-preserved features (G1:G2:G3, 21%:43%:36%) compared to BSF (15%:51%:34%) but a similar proportion of degraded (G3) features.

Landsliding posed a major challenge to mapping the continuity of active traces, requiring initial identification of landslide features to distinguish them from tectonic features. Landslides cause four large gaps in mapping the BSF (≥ 2 km), all within the Franciscan assemblage on steep slopes (km 62–64, km 107–109, km 127–129, and km 150–152).

Fault Location from Creep Evidence

Fault creep, the common name for aseismic slip observed along the surface trace of a fault, has now been recognized along many branches and segments of the San Andreas Fault system (Calaveras, Concord, Green Valley, Greenville, Hayward, Imperial, Maacama, northern Rodgers Creek, central San Andreas, Sargent, and Superstition Hills Faults). Galehouse and Lienkaemper (2003) provide a summary of creep in northern California. Until recently, the possible occurrence of creep on the BSF had only been indicated by less than 5 years of observations across the Round Valley segment of the fault on a low-angle trilateration line (Lisowski and Prescott, 1989). The rate (~ 8 mm/yr) was neither well constrained nor supported by additional measurements on that line, because more recent measurements used GPS on different survey marks.

The U.S. Geological Survey (USGS) began monitoring crustal strain and creep near Lake Pillsbury

and elsewhere in 2005 using GPS and alinement-array methods (Murray and others, 2006); currently six alinement arrays cross the BSF, and updates are reported annually in McFarland and others (2009). As yet, estimates of BSF creep rate are available for only two of these arrays: Lake Pillsbury array (3.1 ± 0.4 mm/yr, 2005–2010) and Hunting Creek array (2.9 ± 0.6 mm/yr; 2007–2009).

Unlike the Hayward Fault, few cultural features cross the BSF, so we have few locations where we have demonstrated the occurrence of creep. Where available, we have used these to refine the location of the active trace. In Round Valley, left-stepping en echelon cracks in the pavement of Fairbanks Road appear to indicate creep (km 38.10), and a ranch fence line (km 40.85) of unknown age (a few decades; fence built the by previous owner) has a distinct right-lateral offset (surveyed at 140 ± 48 mm; Lienkaemper and Brown, 2009). At Lake Pillsbury at the location of the alinement array (km 80.89), left-stepping en echelon cracks form in the pavement and grow noticeably with each creep event (Forrest McFarland, written commun., 2010).

Fault Location from Trenching Evidence

One trenching study on the BSF has been completed by Taylor and Swan (1986): four trench exposures in Gravelly Valley (km 79–81) across the main fault trace and one across a major secondary normal fault that bounds the northeast edge of the Pillsbury Basin, the Sunset Point Lineament. Evidence collected in the trenches demonstrated repeated fault movement in the late Holocene on the main trace and at least late Pleistocene movement on the secondary fault. However, the geomorphic features on the secondary fault are sufficiently well defined to indicate Holocene movement. Taylor and Swan (1986) indicated only the approximate locations of these trenches on a regional map, so their positions are poorly known. Bryant (1993) and CGS (2002) show these approximate locations, but we were not able to verify them for this study.

Acknowledgments

Pacific Gas and Electric (PG&E)-USGS CRADA Task C1213 funded aerial photography and general support. Special thanks go to William D. Page, Scott Steinberg, and Stuart Nishenko of PG&E, who made available the 1985 aerial photos, unpublished reports, and other information relevant to the BSF. Johnathan Brown of San Francisco State University assisted in acquiring aerial photography. We also thank Ben Fetzer of Masut Ranch for allowing access to the fault. Reviews by John Tinsley and J. Luke Blair improved the writing and metadata accompanying this map.

References Cited

- Bryant, W.A., 1982, Hunting Creek fault, Napa, Lake, and Yolo Counties: California Division of Mines and Geology Open-File Report 90-10, Fault Evaluation Report 137 (available as part of CGS, 2002), 8 p., scale 1:24,000.
- Bryant, W.A., 1983, Hunting Creek fault, Lake, Napa, and Yolo Counties: California Division of Mines and Geology Open-File Report 90-10, Fault Evaluation Report FER-137 (microfiche copy), Supplement No. 1, 7 p.
- Bryant, W.A., 1993, Bartlett Springs fault zone, Lake and Mendocino Counties, California: California Division of Mines and Geology Fault Evaluation Report FER-236, (available as part of CGS, 2002), scale 1:24,000.
- Bryant, W.A., comp., 2000, Fault number 29a, Bartlett Springs Fault System, Lake Mountain section, in Quaternary fault and fold database of the United States: U.S. Geological Survey website, <http://earthquake.usgs.gov/regional/qfaults> (accessed 5/13/2010).
- CGS, 2002, Fault evaluation reports (FERs) prepared under the Alquist-Priolo Earthquake Fault Zoning Act, Region 1, Central California: California Geological Survey, v. 2002-1, 6-CD set.
- Daly, C., and Taylor, G., 2000, United States average annual precipitation, 1961–1990 (map layer), in U.S. National Atlas, <http://nationalatlas.gov/mld/prism0p.html> (accessed 4/30/10).
- Galehouse, J.S., and Lienkaemper, J.J., 2003, Inferences drawn from two decades of alinement array measurements of creep on faults in the San Francisco Bay region: *Bulletin of the Seismological Society of America*, v. 93, no. 6, p. 2415–2433.
- Taylor, C.L., and Swan, F.H., 1986, Geological assessment of the seismic potential of the Bartlett Springs shear zone for Scott Dam, Lake County, California: Final report by Geomatrix Consultants for Pacific Gas and Electric Company, San Francisco, California, 51 p.
- Herd, D.G., 1978, Intercontinental plate boundary east of Cape Mendocino, California: *Geology*, v. 6, no. 12, p. 721–725.
- Jayko, A.S., Blake, M.C., Jr., McLaughlin, R.J., Ohlin, H.N., Ellen, S.D., and Kelsey, Harvey, 1989, Reconnaissance geologic map of the Covelo 30- by 60-minute quadrangle, northern California: U.S. Geological Survey Miscellaneous Field Studies MF-2001, scale 1:100,000.
- Lienkaemper, J.J., 1992, Map of recently active traces of the Hayward fault, Alameda and Contra Costa Counties, California: U.S. Geological Survey Miscellaneous Field Studies Map MF-2196, map scale 1:24,000, p. 13.
- Lienkaemper, J.J., 2006, Digital database of recently active traces of the Hayward Fault, California: U.S. Geological Survey Data Series 177, version 1.1 (2008), <http://pubs.usgs.gov/ds/2006/177/> (accessed 4/22/2010).
- Lienkaemper, J., and Brown, J., 2009, Preliminary investigation of factors affecting the seismic potential of the Bartlett Springs fault zone, northern California: American Geophysical Union, Fall Meeting 2009, abstract #S51B-1403.
- Lisowski, M., and Prescott, W.H., 1989, Strain accumulation near the Mendocino triple junction [abs.]: *Eos, Transactions of the American Geophysical Union*, v. 70, no. 43, p. 1332.
- Lock, J., Kelsey, H., Furlong, K., and Woolace, A., 2006, Late Neogene and Quaternary landscape evolution of the northern California Coast Ranges—Evidence for Mendocino triple junction tectonics: *Geological Society of America Bulletin*, v. 118, no. 9/10, p. 1232–1246.
- McFarland, F.S., Lienkaemper, J.J., and Caskey, S.J., 2009, Data from theodolite measurements of creep rates on San Francisco Bay region faults, California, 1979–2009: U.S. Geological Survey Open-File Report, 2009-1119, version 1.1 (2010), p. 17. <http://pubs.usgs.gov/of/2009/1119/> (accessed 5/5/10).
- McLaughlin, R.J., Ohlin, H.N., Thormahlen, D.J., Jones, D.L., Miller, J.W., and Blome, C.D., 1990, Geologic map and structure sections of the Little Indian Valley-Wilbur Springs geothermal area, northern Coast Ranges, California: U.S. Geological Survey Miscellaneous Investigations Series Map I-1706, scale 1:24,000.
- Muir, K.S., and Webster, D.A., 1977, Geohydrology of part of the Round Valley Indian Reservation, Mendocino County, California: U.S. Geological Survey Water-Resources Investigations Report 77-22, 40 p.
- Murray, J., Svarc, J., Lienkaemper, J., Langbein, J., McFarland, F., Nishenko, S., and Page, W., 2006, A new campaign GPS network and alinement array on the Bartlett Springs Fault: *Seismological Research Letters*, v. 77, p. 202.

- Ohlin, H.N., McLaughlin, R.J. and Moring, B.C., 2010, Geologic map of the Bartlett Springs Fault Zone in the vicinity of Lake Pillsbury and adjacent areas of Mendocino, Lake, and Glenn County, California, U.S. Geological Survey Open-file Report 2010-1301 scale 1:24,000.
- Sharp, 1972, Map showing recently active breaks along the San Jacinto Fault Zone between the San Bernardino area and Borrego Valley, California: U.S. Geological Survey Miscellaneous Investigations Map I-675, scale 1:24,000, 3 sheets.
- USGS and CGS, 2006, Quaternary fault and fold database for the United States: U.S. Geological Survey and California Geological Survey, <http://earthquake.usgs.gov/regional/qfaults/> (accessed 5/13/2010).
- Wallace, R.E., 1990, Geomorphic expression, in Wallace, R.E., ed., The San Andreas Fault System, California: U.S. Geological Survey Professional Paper 1515, p. 14–58.
- Wallace, R.E., ed., 1990, The San Andreas Fault System, California: U.S. Geological Survey Professional Paper 1515, 283 p.
- Wesnousky, S.G., 2008, Displacement and geometrical characteristics of earthquake surface ruptures—Issues and implications for seismic-hazard analysis and the process of earthquake rupture: Bulletin of Seismological Society of America, no. 98, p. 1609–1632.

Table 1. Major right-lateral stream offsets (>0.5 km) along the Bartlett Springs Fault (BSF), northern California.

Kilometer grid value (km #) along BSF	Slip (km)	Location	Notes
15.62	1.0±0.1	North Fork Eel River	
24.20	>1.25±0.25	Mud Creek	Minimum estimate, head and tail misaligned
27.00	1.1±0.1	Alder Creek	
32.40	1.0±0.1	Town Creek	Sum of slip on two traces
44.70	6.6±0.2	Middle Fork Eel River	
84.00	5.0±0.5	Eel River	Offset zone broadened by uplift of McLeod Ridge
89.90	2.0±0.2	Deer Creek	
92.75	1.0±0.1	Rice Creek	
96.90	1.1±0.1	Bear Creek	Older, highly eroded offset (see table 2)
101.10	2.5±0.5	Rice Fork Eel River	
109.10	0.7±0.1	North Fork Cache Creek	
110.70	1.2±0.1	Soap Creek	
116.65	4.9±0.1	Bartlett Creek	
133.16	1.5±0.1	North Fork Cache Creek	Lower crossing of creek on two fault strands
139.70	0.7±0.1	Indian Creek	
143.10	0.9±0.1	Grizzly Creek	
146.00	6.2±0.2	Cache Creek	

Table 2. Minor right-lateral stream offsets (≤ 500 m) along the Bartlett Springs Fault (BSF), northern California.

Kilometer grid value (km #) along BSF	Slip (m)	Location	Notes
38.76	110 \pm 10	unnamed creek	
52.62	30 \pm 10	near Elk Creek	
57.60	50 \pm 10	near Elk Creek	
57.70	50 \pm 10	near Elk Creek	
57.90	$\leq 10\pm 5$	near Elk Creek	
58.28	135 \pm 5	near Elk Creek	
58.60	40 \pm 10	near Elk Creek	
60.42	80 \pm 20	near Elk Creek	
61.40	160 \pm 10	near Elk Creek	
95.30	500 \pm 100	unnamed creek	
96.90	250 \pm 50	Bear Creek	Youngest, most distinct part of offset
98.60	250 \pm 50	unnamed creek	
121.90	25 \pm 5	near Reister Rock	
122.30	100 \pm 10	near Reister Rock	
124.40	25 \pm 5	near Reister Rock	
126.50	160 \pm 10	near Reister Knoll	
131.80	100 \pm 10	near Panther Canyon	
138.00	>70 \pm 10	Benmore Canyon	On one of two traces
139.50	210 \pm 10	near Indian Creek	
141.40	40 \pm 10	Middle Creek	
142.60	50 \pm 5	unnamed creek	Distinct, on one of two traces
142.80	30 \pm 5	unnamed creek	Distinct, on one of two traces
146.70	65 \pm 5	unnamed creek	Distinct offset
147.80	240 \pm 10	Rocky Creek	
153.70	500 \pm 50	near Buck Mountain	
154.80	200 \pm 10	unnamed creek	
163.10	190 \pm 10	unnamed creek	
164.50	200 \pm 20	Hunting Creek	
168.65	80 \pm 5	Cedar Creek	

Appendix

Map Abbreviations

G1	strongly pronounced feature
G2	distinct feature
G3	weakly pronounced feature
?	additional uncertainty in tectonic origin
af	alignment of multiple features as listed
as	arcuate scarp
bfs	back-facing scarp
bt	downthrown surface tilts back toward fault
dd	deflected drainage
df	depression formed by some aspect of fault deformation, undifferentiated
dr	sag, depression formed in right stepover of fault trace
ec	en echelon cracks in pavement, evidence of creep
fs	faceted spur
gi	linear break (or gradual inflection) in slope
hb	linear hillside bench
hv	linear hillside valley
lr	linear ridge
ls	fault scarp height enlarged by landsliding
lv	linear valley or trough
mp	Youngest traces disturbed by human activities. Mapped trace bisects disturbed zone. Location uncertainty (dash gap in linework) equals half width of disturbed zone.
n	notch
pr	pressure ridge in left stepover
rr	right-laterally offset ridge line
rs	right-laterally offset stream or gully
s	saddle
sb	broad linear scarp (implies multiple traces)
sc	scissor point, sense of vertical separation reverses
se	subsoil exposed
sn	narrow linear scarp (implies dominant trace)
sp	spring
ss	swale in saddle
vl	line of vegetation
